

# SWARM INTELLIGENCE BASED OPTIMAL DESIGN OF CONCENTRIC CIRCULAR ANTENNA ARRAY

**Durbadal MANDAL Anup Kumar BHATTACHARJEE**

National Institute of Technology Durgapur  
Electronics and Communication Engineering Department, West Bengal, India- 713209  
Tel.: +91 343 2545021; Fax: +91 343 2547375; E-mail address: [durbadal.bittu@gmail.com](mailto:durbadal.bittu@gmail.com)

**Sakti Prasad GHOSHAL**

National Institute of Technology Durgapur  
Department of Electrical Engineering, West Bengal, India- 713209  
Tel.: +91 343 2547231; Fax: +91 343 2547375; E-mail address: [spghoshalnidgp@gmail.com](mailto:spghoshalnidgp@gmail.com)

**Abstract:** In this paper the maximum sidelobe level (SLL) reductions for various designs without and with central element feeding in three-ring concentric circular antenna arrays (CCAA) are examined using two novel variants of particle swarm optimization techniques as (i) an improved particle swarm optimization technique (IPSO) and (ii) a novel particle swarm optimization technique (NPSO) to finally determine the global optimal three-ring CCAA design. Real coded Genetic Algorithm (RGA) is also employed for comparative optimization but it proves to be suboptimal. Among the various CCAA designs, the design containing 4, 6 and 8 elements along with central element feeding in three successive concentric rings proves to be such global optimal design with minimum SLL (-36.80 dB) determined by IPSO and (-39.38 dB) determined by NPSO.

**Key words:** concentric circular antenna array, non-uniform excitation, sidelobe level, real coded genetic algorithm, particle swarm optimization

## 1. Introduction

An antenna array consists of multiple stationary antenna elements, which are often fed coherently. There are abundant open technical literatures [1-12], bearing a common target - bridging the gap between desired radiation pattern having nil SLL with what is practically achievable. The primary method in all these research works is improvement of array pattern by manipulating the structural geometry to suppress the SLL while preserving the gain of the main beam. Among the different structures of antenna arrays, CCAA [1, 6] have become most popular in mobile, and wireless communications, radar and sonar [7, 8].

In this paper optimization is performed for non-uniform current excitation weights in various CCAA design sets each having uniform element separation. For optimization, two variants of Particle Swarm Optimization algorithms (IPSO and NPSO) [13-17] and conventional Real coded Genetic Algorithm (RGA) [9, 11] are adopted. The array factors due to

optimal current excitation weights in various CCAA design sets are examined to find the best possible design set.

Regarding the comparative optimization effectiveness of the techniques, the proposed NPSO technique proves to be the best in attaining minimum SLL, reduction of major lobe beamwidth and hence near global minimum "Misfitness" objective function value in the optimization of each CCAA design.

The rest of the paper is arranged as follows: In section 2, the general design equations for the non-uniformly excited CCAA are stated. Then, in section 3, brief introductions for the RGA, IPSO and NPSO are presented. Convergence test of optimization Techniques are discussed in section 4. Numerical results are presented in section 5. Finally the paper concludes with a summary of the work in section 6.

## 2. Design Equation

Geometrical configuration is a key factor in the design process of an antenna array. For CCAA, the elements are arranged in such a way that all antenna elements are placed in multiple concentric circular rings, which differ in radii and in number of elements. Fig. 1 shows the general configuration of CCAA with  $M$  concentric circular rings, where the  $m^{\text{th}}$  ( $m = 1, 2, \dots, M$ ) ring has a radius  $r_m$  and the corresponding number of elements is  $N_m$ . If all the elements (in all the rings) are assumed to be isotropic sources, then the radiation pattern of this array can be expressed in terms of its array factor only.

Referring to Fig.1, the array factor,  $AF(\phi, I)$  for the CCAA in  $x$ - $y$  plane is expressed as:

$$AF(\phi, I) = \sum_{m=1}^M \sum_{i=1}^{N_m} I_{mi} \exp[j(Kr_m \sin \theta \cos(\phi - \phi_{mi}) + \alpha_{mi})] \quad (1)$$

where  $I_{mi}$  denotes current excitation of the  $i^{\text{th}}$  element of the  $m^{\text{th}}$  ring,  $K = 2\pi/\lambda$ ;  $\lambda$  being the signal

wave-length, and  $\theta$  and  $\phi$  symbolize the zenith angle from the positive  $z$  axis and the azimuth angle from the positive  $x$  axis to the orthogonal projection of the observation point respectively. It may be noted that if the elevation angle is assumed to be  $90^\circ$  i.e.  $\theta = 90^\circ$  then (1) may be written as a periodic function of  $\phi$  with a period of  $2\pi$  radian. The angle  $\phi_{mi}$  is nothing but element to element angular separation measured from the positive  $x$ -axis. As the elements in each ring are assumed to be uniformly distributed,  $\phi_{mi}$  may be written as:

$$\phi_{mi} = 2\pi \left( \frac{i-1}{N_m} \right); \quad m = 1, \dots, M; \quad i = 1, \dots, N_m \quad (2)$$

The residual phase term  $\alpha_{mi}$  is a function of angular separation  $\phi_{mi}$  and ring radii  $r_m$ .

$$\alpha_{mi} = -Kr_m \cos(\phi_0 - \phi_{mi}); \quad m = 1, \dots, M; \quad i = 1, \dots, N_m \quad (3)$$

where  $\phi_0$  is the value of  $\phi$  where peak of the main lobe is obtained.

After defining the array factor, the next step in the design process is to formulate the objective function which is to be minimized. The objective function ‘‘Misfitness’’ ( $MF$ ) may be written as (4):

$$MF = W_{F1} \times \frac{|AF(\phi_{msl1}, I_{mi}) + AF(\phi_{msl2}, I_{mi})|}{|AF(\phi_0, I_{mi})|} + W_{F2} \times (BWFN_{computed} - BWFN(I_{mi} = 1)) \quad (4)$$

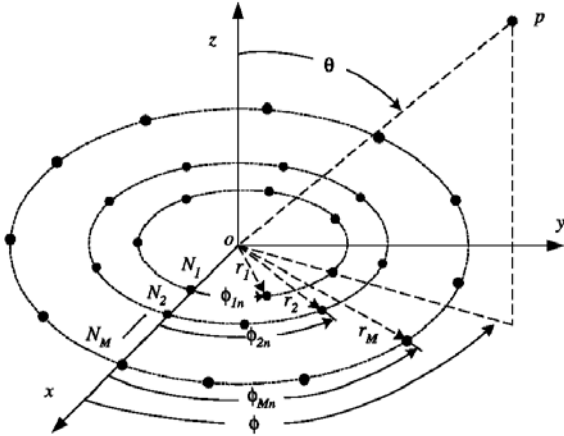


Fig. 1. Concentric circular antenna array (CCAA).

$BWFN$  is an abbreviated form of first null beamwidth, or, in simple terms, angular width between the first nulls on either side of the main beam.  $MF$  is computed only if  $BWFN_{computed} < BWFN(I_{mi} = 1)$  and corresponding solution of current excitation weights is retained in the active population otherwise not retained.  $W_{F1}$  (*unitless*) and  $W_{F2}$  (*radian<sup>-1</sup>*) are the weighting factors.  $\phi_0$  is the angle where the highest maximum of central lobe is attained in  $\phi \in [-\pi, \pi]$ .  $\phi_{msl1}$  is the

angle where the maximum sidelobe ( $AF(\phi_{msl1}, I_{mi})$ ) is attained in the lower band and  $\phi_{msl2}$  is the angle where the maximum sidelobe ( $AF(\phi_{msl2}, I_{mi})$ ) is attained in the upper band.  $W_{F1}$  and  $W_{F2}$  are so chosen that optimization of SLL remains more dominant than optimization of  $BWFN_{computed}$  and  $MF$  never becomes negative. In (4) the two beamwidths,  $BWFN_{computed}$  and  $BWFN(I_{mi} = 1)$  basically refer to the computed first null beamwidths in radian for the non-uniform excitation case and for uniform excitation case respectively. Minimization of  $MF$  means maximum reductions of SLL both in lower and upper sidebands and lesser  $BWFN_{computed}$  as compared to  $BWFN(I_{mi} = 1)$ . The evolutionary optimization techniques employed for optimizing the current excitation weights resulting in the minimization of  $MF$  and hence reductions in both SLL and  $BWFN$  are described in the next section.

### 3. Evolutionary Techniques Employed

#### 3. A. Real Coded Genetic Algorithm (RGA)

GA is mainly a probabilistic search technique, based on the principles of natural selection and evolution. Steps of RGA [9, 11] as implemented for optimization of current excitation weights are:

- Initialization of real chromosome strings of  $n_p$  population, each consisting of a set of current excitation weights. Size of the set depends on the number of excitation elements in a particular CCAA design
- Decoding of strings and evaluation of  $MF$  of each string
- Selection of elite strings in order of increasing  $MF$  values from the minimum value
- Copying of the elite strings over the non-selected strings
- Crossover and mutation to generate off-springs
- Genetic cycle updating

The genetic cycle stops when the maximum number of cycles is reached. The grand minimum  $MF$  and its corresponding chromosome string having the desired current excitation weights are finally obtained.

#### 3. B. Particle Swarm Optimization (PSO)

PSO is a flexible, robust population-based stochastic search/optimization technique with implicit parallelism, which can easily handle with non-differential objective functions, unlike traditional optimization methods. PSO is less susceptible to

getting trapped on local optima unlike GA, Simulated Annealing etc. Eberhart and Shi [13] developed PSO concept similar to the behavior of a swarm of birds. PSO is developed through simulation of bird flocking in multidimensional space. Bird flocking optimizes a certain objective function. Each particle (bird) knows its best value so far (pbest). This information corresponds to personal experiences of each particle. Moreover, each particle knows the best value so far in the group (gbest) among pbests. Namely, each particle tries to modify its position using the following information:

- The distance between the current position and the pbest.
- The distance between the current position and the gbest.

Similar to GA, in PSO techniques also, real particle vectors of population  $n_p$  are assumed. Each particle vector consists of components like required number of current excitation weights, depending on the number of excitation elements in each CCAA design.

Mathematically, velocities of the particles are modified according to the following equation:

$$V_i^{(k+1)} = w * V_i^k + C_1 * rand_1 * (pbest_i^k - S_i^k) + C_2 * rand_2 * (gbest^k - S_i^k) \quad (5)$$

where  $V_i^k$  is the velocity of  $i^{th}$  particle at  $k^{th}$  iteration;  $w$  is the weighting function;  $C_1$  and  $C_2$  are the positive weighting factors;  $rand_1$  and  $rand_2$  are the random numbers between 0 and 1;  $S_i^k$  is the current position of  $i^{th}$  particle at  $k^{th}$  iteration;  $pbest_i^k$  is the personal best of  $i^{th}$  particle at  $k^{th}$  iteration;  $gbest^k$  is the group best of the group at  $k^{th}$  iteration. The searching point in the solution space may be modified by the following equation:

$$S_i^{(k+1)} = S_i^k + V_i^{(k+1)} \quad (6)$$

The first term of (5) is the previous velocity of the particle. The second and third terms are used to change the velocity of the particle. Without the second and third terms, the particle will keep on ‘‘flying’’ in the same direction until it hits the boundary. Namely, it corresponds to a kind of inertia represented by the inertia constant,  $w$  and tries to explore new areas.

### 3. B. i. Improved Particle Swarm Optimization (IPSO)

The global search ability of traditional PSO is very much enhanced with the help of the following modifications. This modified PSO is termed as IPSO [16].

i) The two random parameters  $rand_1$  and  $rand_2$  of (5) are independent. If both are large, both the personal

and social experiences are over used and the particle is driven too far away from the local optimum. If both are small, both the personal and social experiences are not used fully and the convergence speed of the technique is reduced. So, instead of taking independent  $rand_1$  and  $rand_2$ , one single random number  $r_1$  is chosen so that when  $r_1$  is large,  $(1-r_1)$  is small and vice versa. Moreover, to control the balance of global and local searches, another random parameter  $r_2$  is introduced. For birds flocking for food, there could be some rare cases that after the position of the particle is changed according to (6), a bird may not, due to inertia, fly toward a region at which it thinks is the most promising for food. Instead, it may be leading toward a region which is in the opposite direction of what it should fly in order to reach the expected promising regions. So, in the step that follows, the direction of the bird’s velocity should be reversed in order for it to fly back into the promising region.  $sign(r_3)$  is introduced for this purpose. Both cognitive and social parts are modified accordingly.

Finally, the modified velocity of  $j^{th}$  component of  $i^{th}$  particle is expressed as follows:

$$V_i^{(k+1)} = r_2 * sign(r_3) * V_i^k + (1-r_2) * C_1 * r_1 * \{pbest_i^k - S_i^k\} + (1-r_2) * C_2 * (1-r_1) * \{gbest^k - S_i^k\} \quad (7)$$

where  $r_1$ ,  $r_2$  and  $r_3$  are the random numbers between 0 and 1;  $S_i^k$  is the current position of particle  $i$  at iteration  $k$ ;  $pbest_i^k$  is the personal best of  $i^{th}$  particle at  $k^{th}$  iteration;  $gbest^k$  is the group best among all pbests for the group at  $k^{th}$  iteration. The searching point in the solution space can be modified by the following equation (6).

$sign(r_3)$  is a function defined as:

$$sign(r_3) = -1 \text{ when } r_3 \leq 0.05, \\ = 1 \text{ when } r_3 > 0.05. \quad (8)$$

### 3. B. ii. Novel Particle Swarm Optimization (NPSO)

The search ability of IPSO is further enhanced with the help of the following modification. This modified PSO is named as NPSO [17].

i) A new variation in the velocity expression (5) is made by splitting the cognitive component (second part of (5)) into two different components. The first component can be called good experience component. That is, the particle has a memory about its previously visited best position. This component is exactly the same as the cognitive component of the basic PSO. The second component is given the name bad experience component. The bad

experience component helps the particle to remember its previously visited worst position. The inclusion of the worst experience component in the behavior of the particle gives additional exploration capacity to the swarm. By using the bad experience component, the bird (particle) can bypass its previous worst position and always try to occupy a better position.

Finally, with all modifications, the modified velocity of  $j^{\text{th}}$  component of  $i^{\text{th}}$  particle is expressed as follows:

$$V_i^{(k+1)} = r_2 * \text{sign}(r_3) * V_i^k + (1-r_2) * C_1 * r_1 * \{pbest_i^k - S_i^k\} + (1-r_2) * C_2 * (1-r_1) * \{gbest^k - S_i^k\} + (1-r_2) * c_1 * r_1 (S_i^k - pworst_i^k) \quad (9)$$

where  $pworst_i^k$  are the personal best and the personal worst of particle  $i$  respectively ; the other notations are already mentioned in the explanation of IPSO.

## 4. Convergence Tests of Optimization Techniques

### 4.1. Benchmark Test Functions

A suite of six benchmark test functions [18-19]: Sphere model ( $f_1$ ), Generalized Rosenbrock's function( $f_2$ ), Maxican hat function( $f_3$ ), Six-hump camel back function( $f_4$ ), Generalized Rastrigin's function( $f_5$ ) and Generalized Griewank function( $f_6$ ) are used to test the performances of the optimization techniques. Some of these functions are plotted in Figs. 2-4 for  $N = 2$  for ease of visualization. Many different kinds of optimization problems are tested by these benchmark test functions. They are divided into three categories: unimodal functions, multimodal functions with only a few local minima and multimodal functions with many local minima. They can test the searching ability of the optimization techniques comprehensively.

#### A. Unimodal Function

##### i) Generalized Rosenbrock function:

The very narrow ridge in this function makes the landscape more complicated and difficult to be explored. Algorithms that are unable to discover good directions do not perform well on this problem.

$$f_2(x) = \sum_{i=1}^N (100(x_{i+1} - x_i^2)^2 + (x_i - 1)^2) \quad (10)$$

where

$x=[x_1, x_2, \dots, x_N]$  is a N-dimensional real-valued vector.

#### B. Multimodal Functions with Many Local Minima

##### i) Generalized Rastrigin function:

This function contains millions of local optima in the interval of consideration, making it a fairly difficult

problem of optimization. The function is highly multimodal.

$$f_5(x) = \sum_{i=1}^N (x_i^2 - 10 \cos(2\pi x_i) + 10) \quad (11)$$

where

$x=[x_1, x_2, \dots, x_N]$  is a N-dimensional real-valued vector.

##### ii) Generalized Griewank function:

The function can be defined as

$$f_6 = \frac{1}{4000} \sum_{i=1}^N x_i^2 - \prod_{i=1}^N \cos\left(\frac{x_i}{\sqrt{i}}\right) + 1 \quad (12)$$

where

$x=[x_1, x_2, \dots, x_N]$  is a N-dimensional real-valued vector.

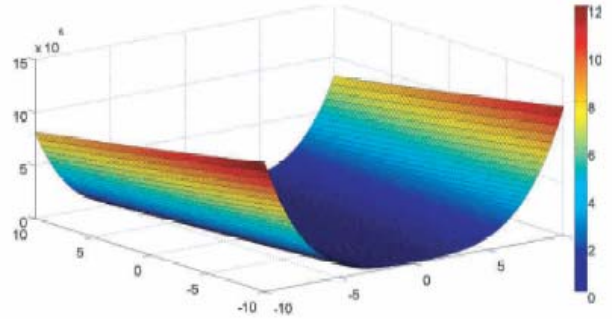


Fig. 2. Plot of Generalized Rosenbrock function ( $f_2$ ).

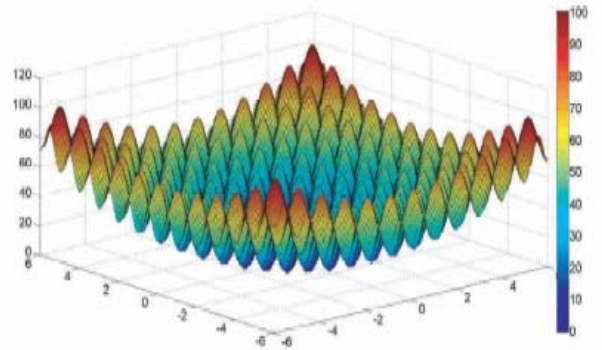


Fig. 3. Plot of Generalized Rastrigin function ( $f_5$ ).

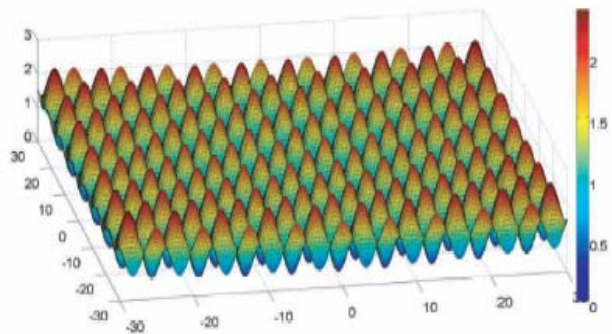


Fig. 4. Plot of Generalized Griewank function ( $f_6$ ).

## 4.2. Test Results

Table 1 shows the asymmetric initialization ranges for the functions ( $f_2$ ,  $f_5$  and  $f_6$ ). Table 2 portrays the comparative performances of the optimization techniques tested on the above three functions respectively. The convergence profiles obtained by the techniques are displayed in Figs. 5-7.

Table 1

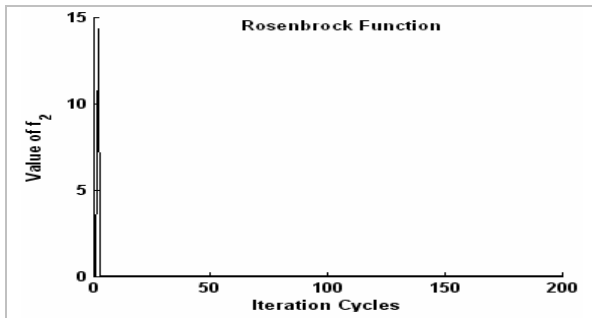
Asymmetric initialization ranges for different benchmark functions [23]

Function	Dimension	Asymmetric initialization ranges
$f_2$	2	$(0.1, 2.048)^N$
$f_5$	2	$(0.1, 10.24)^N$
$f_6$	2	$(0.1, 600)^N$

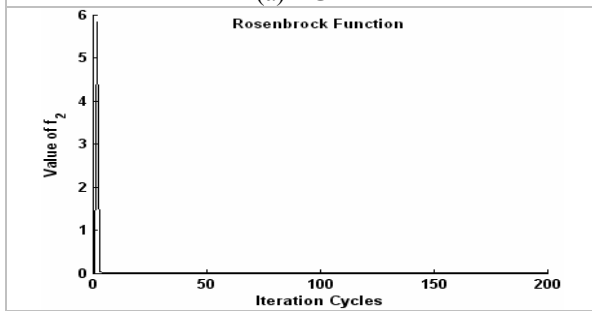
Table 2

Computational results for Rosenbrock, Generalized Rastrigrin and Griewank functions

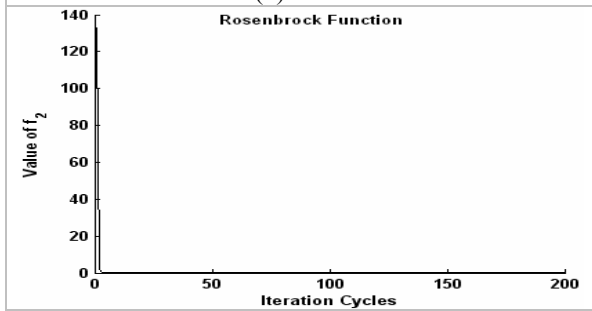
Function	Technique	Desired min	Computed min	Parameters	Execution time (Sec)
$f_2$	RGA	0.0000	0.0374	1.0456, 1.1467	5.6784
	IPSO		0.0169	1.0329, 1.0241	4.2500
	NPSO		0.0030	0.9455, 0.8947	7.6100
$f_5$	RGA	2.0000	2.0305	0.9960, 1.0014	0.9690
	IPSO		1.9967	0.9934, 1.0006	0.6870
	NPSO		2.0000	1.0000, 1.0000	1.2500
$f_6$	RGA	0.0075	0.0075	0.1000, 0.1000	1.0875
	IPSO		0.0075	0.1000, 0.1000	0.7840
	NPSO		0.0075	0.1000, 0.1000	1.8280



(a) RGA

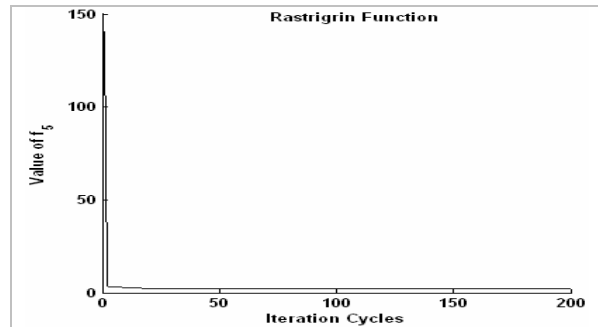


(b) IPSO

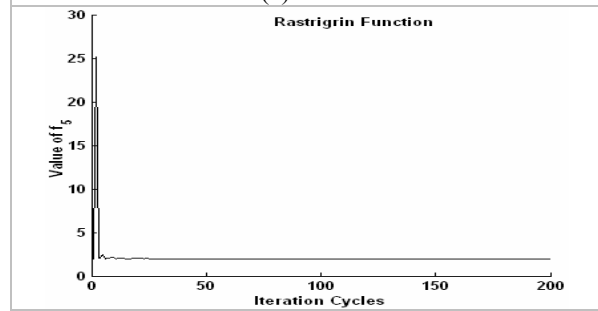


(c) NPSO

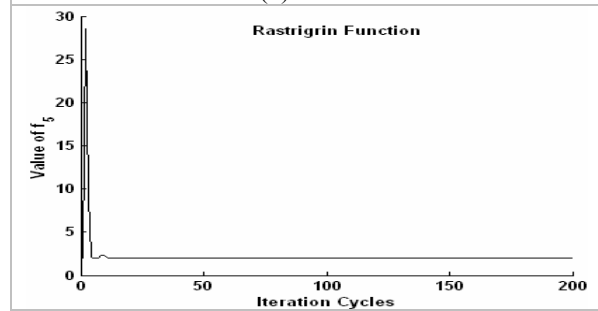
Fig. 5. Convergence characteristics for different techniques for Rosenbrock function.



(a) RGA



(b) IPSO



(c) NPSO

Fig. 6. Convergence characteristics for different techniques for Rastrigrin function.

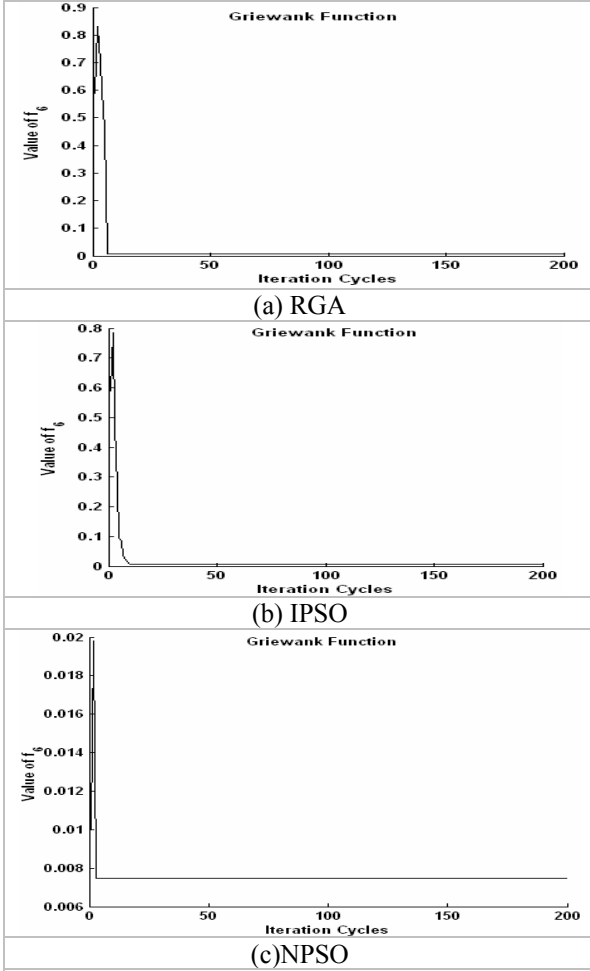


Fig. 7. Convergence characteristics for different techniques for Griewank function.

## 5. Computational results

This section gives the computational results for various CCAA design sets obtained by RGA, IPSO and NPSO techniques. For each optimization technique ten three-ring ( $M=3$ ) CCAA sets for each case, (a) without central element feeding and (b) with central element feeding in three-ring concentric circular antenna arrays (CCAA) are assumed. Each CCAA maintains a fixed spacing between the elements in each ring (inter-element spacing for: first ring =  $0.55\lambda$ , second ring =  $0.61\lambda$  and third ring =  $0.75\lambda$ ). These spacings are the means of the values determined for the ten sets for non-uniform spacing and non-uniform current excitation weights in each ring using 25 trial generalized optimization runs for each set. For all sets of experiments, the number of elements for the inner-most ring, the middle ring and the outermost ring are  $N_1$ ,  $N_2$  and  $N_3$  respectively. For all the cases,  $\phi_0 = 0^\circ$  is considered so that the centre of the main lobe in radiation patterns of CCAA starts from the origin. After experimentation, best proven values of weighting factors,  $W_{F1}$  and  $W_{F2}$  of (4) are fixed as 18 and 1 respectively.

The following best proven parameters for the RGA and the two PSOs are: i) Initial population = 120 chromosomes, ii) Maximum number iteration cycles = 400 (RGA), 100 (IPSO, NPSO); lesser number of cycles is found to be sufficient for the convergence of the two PSOs, since PSO's convergence rate is higher than RGA's convergence rate, iii) For RGA, Selection probability, Crossover (random dual point) ratio and mutation probability = 0.3, 0.8 and 0.004 respectively, iv) For the PSOs,  $C_1 = C_2 = 1.5$ .

Each RGA, IPSO and NPSO technique generates a set of normalized optimal non-uniform current excitation weights for each set of CCAA.  $I_{mi}=1$  corresponds to uniform current excitation. Sets of three-ring CCAA ( $N_1, N_2, N_3$ ) designs considered for both without and with central element feeding are (2, 4, 6), (3,5,7), (4,6,8), (5,7,9), (6,8,10), (7,9,11), (8,10,12), (9,11,13), (10,12,13), (11,13,15). Three sets of optimal results for each RGA, IPSO and NPSO are shown in Tables 4-9. Table 3 depicts SLL values and *BWFN* values for all corresponding uniformly excited CCAA sets.

### 5. A. Analysis of radiation pattern of optimal CCAA

Figs. 8-10 depict the substantial reductions in SLL with non-uniform optimal excitation weights as compared to the case of uniform non-optimal current excitation weights. All three techniques yield much more reductions in SLL for all CCAA design sets with central element feeding as compared to the same without central element feeding. As seen from Tables 4-9 SLL reduces to -28.06 dB (RGA), -30.94 dB (IPSO), -32.90 dB (NPSO) for Case (a) (Set III) and -34.32 dB (RGA), -36.80 dB (IPSO), **-39.38 dB (grand highest SLL reduction as determined by NPSO)** for Case (b) (shown as a shaded row in Table 9) with the CCAA set having  $N_1=4, N_2=6, N_3=8$  elements (Set III). This optimal set yields grand maximum SLL reductions for all three techniques among all the sets. IPSO and NPSO yield more reductions in SLL than RGA for each CCAA set without and with central element feeding.

*BWFN* also become narrower for non-uniform optimal current excitation weights as compared to the uniform non-optimal excitations in all cases. For the same optimal CCAA set, the *BWFN* values are  $77.1^\circ$  (RGA),  $77.0^\circ$  (IPSO), and  $76.0^\circ$  (NPSO) for Case (a),  $84.0^\circ$  (RGA),  $82.8^\circ$  (IPSO) and  $87.3^\circ$  (NPSO) for Case (b) against  $90.3^\circ$  (Case (a)),  $95.4^\circ$  (Case (b)) for the corresponding uniformly excited CCAA having the same number of elements. So, these techniques yield maximum reductions of *BWFN* also for this optimal CCAA.

Table 3  
SLL and BWFN for uniformly excited ( $I_{mi}=1$ ) CCAA

Set No.	No. of elements in each rings ( $N_1, N_2, N_3$ )	Without central element (Case (a))		With central element (Case (b))	
		SLL (dB)	BWFN (deg)	SLL (dB)	BWFN (deg)
I	2, 4, 6	-12.56	128.4	-17.0	140.0
II	3, 5, 7	-13.8	107.2	-15.0	116
III	4, 6, 8	-11.23	90.3	-12.32	95.4
IV	5, 7, 9	-11.2	78.2	-13.24	81.6
V	6, 8, 10	-10.34	68.4	-12.0	71.1
VI	7, 9, 11	-10.0	61.0	-11.32	63.0
VII	8, 10, 12	-9.6	54.8	-10.76	56.4
VIII	9, 11, 13	-9.28	50.0	-10.34	51.3
IX	10, 12, 14	-9.06	46.0	-10.0	47.0
X	11, 13, 15	-8.90	42.0	-9.8	43.2

Table 4  
Current excitation weights, SLL and BWFN for optimal, non-uniformly excited CCAA (Case (a)) using RGA

Set No.	Current excitation weights for the array elements ( $I_{11}, I_{12}, \dots, I_{mi}$ )										MF	SLL (dB)	BWFN (deg)
III	0.3773	0.9491	0.3830	0.7861	0.5661	0.6932	0.9638	0.6275	0.5465	0.9349	1.57	-28.06	77.1
	0.4878	0.7220	0.5123	0.2850	0.6041	0.7300	0.5016	0.2799					
V	0.5513	0.4810	0.6504	0.5254	0.7093	0.9878	0.9240	0.0206	0.7129	0.9853	1.99	-25.3	59.6
	0.8481	0.0006	0.8226	0.9933	0.4945	0.7770	0.6438	0.4928	0.6184	0.4075			
	0.9723	0.8552	0.4231	0.5006									
VII	0.7507	0.3438	0.7676	0.9471	0.8357	0.4322	0.8105	0.9816	0.4392	0.1996	1.50	-26.24	51.8
	0.2429	0.8479	0.5903	0.6827	0.0409	0.0649	0.9464	0.5148	0.5861	0.0744			
	0.9357	0.3858	0.4818	0.4177	0.2614	0.5137	0.9845	0.6134	0.3000	0.5170			

Table 5  
Current excitation weights, SLL and BWFN for optimal, non-uniformly excited CCAA (Case (b)) using RGA

Set No.	Current excitation weights for the array elements ( $I_{11}, I_{12}, \dots, I_{mi}$ )										MF	SLL (dB)	BWFN (deg)
III	0.4114	0.6870	0.9740	0.6609	0.9566	0.7231	0.6604	0.8840	0.7331		0.76	-34.32	84.0
	0.6333	0.8109	0.5521	0.7222	0.5261	0.1991	0.6528	0.7360	0.5624				
	0.1988												
V	0.3133	0.6070	0.4469	0.6535	0.5605	0.5371	0.8150	0.8702	0.0191		1.58	-27.52	60.7
	0.7174	0.9248	0.5435	0.0055	0.9165	0.9551	0.2993	0.9178	0.7840				
	0.3256	0.5021	0.3362	0.7293	0.9277	0.4545	0.4949						
VII	0.7336	0.5878	0.8171	0.6285	0.9334	0.5923	0.9541	0.4979	0.9455		1.44	-28.10	55.4
	0.7430	0.0891	0.0076	0.7318	0.4378	0.8178	0.0077	0.0403	0.7994				
	0.5177	0.4003	0.3999	0.8346	0.4101	0.4733	0.4789	0.4304	0.3757				
	0.9218	0.5178	0.2464	0.3176									

Table 6  
Current excitation weights, SLL and BWFN for optimal, non-uniformly excited CCAA (Case (a)) using IPSO

Set No.	Current excitation weights for the array elements ( $I_{11}, I_{12}, \dots, I_{mi}$ )										MF	SLL (dB)	BWFN (deg)
III	0.2627	0.7210	0.2934	0.8062	0.5205	0.4549	0.9229	0.4710	0.5328	1.0000	1.01	-30.94	77.0
	0.5047	0.7571	0.4666	0.2824	0.4476	0.7655	0.4755	0.2603					
V	0.5898	0.4557	0.8915	0.5845	0.5826	0.7157	0.7554	0.0024	1.0000	0.9997	1.79	-26.28	60.0
	0.8149	0.0002	0.6834	0.9960	0.5656	0.7870	0.8495	0.4840	0.3921	0.3375			
	0.8508	0.8327	0.3992	0.5780									
VII	0.8797	0.4214	0.7917	0.8798	0.7259	0.4046	0.7728	0.9795	0.6673	0.2388	1.44	-26.84	51.8
	0.0667	0.6917	0.4563	0.7247	0.0000	0.1562	0.6141	0.4940	0.3613	0.3553			
	0.9702	0.3091	0.4248	0.4615	0.4081	0.4474	0.9148	0.3575	0.3570	0.4125			

Table 7

Current excitation weights, SLL and BWFN for optimal, non-uniformly excited CCAA (Case (b)) using IPSO

Set No.	Current excitation weights for the array elements ( $I_{11}, I_{12}, \dots, I_{mi}$ )									MF	SLL (dB)	BWFN (deg)
III	0.3286	0.5247	0.9394	0.5759	0.9617	0.6526	0.6479	1.0000	0.6603	0.64	-36.8	82.8
	0.6904	0.9415	0.5947	0.7374	0.6044	0.2658	0.5901	0.8050	0.5784			
	0.2282											
V	0.6820	0.6479	0.4552	0.2491	0.3610	0.5122	0.9340	0.8508	0.2413	1.51	-27.6	59.0
	0.4122	1.0000	0.3001	0.2245	0.8157	1.0000	0.3381	1.0000	0.8942			
	0.2727	0.5808	0.3359	0.7631	0.9528	0.3366	0.4732					
VII	0.6323	0.7016	0.6992	0.6429	0.9198	0.5076	0.8026	0.6549	0.9991	1.35	-28.56	54.9
	0.8022	0.0876	0.0364	0.8577	0.5634	0.5816	0.0703	0.1957	0.8024			
	0.5639	0.4077	0.4874	1.0000	0.5435	0.3892	0.4976	0.4542	0.3156			
	0.9996	0.3611	0.4881	0.5881								

Table 8

Current excitation weights, SLL and BWFN for optimal, non-uniformly excited CCAA (Case (a)) using NPSO

Set No.	Current excitation weights for the array elements ( $I_{11}, I_{12}, \dots, I_{mi}$ )									MF	SLL (dB)	BWFN (deg)	
III	0.1352	0.6342	0.1276	0.7173	0.4605	0.3996	0.9999	0.3881	0.4328	0.9999	0.84	-32.90	76.0
	0.4861	0.7093	0.4786	0.2444	0.4951	0.7217	0.5059	0.2206					
V	0.6540	0.3225	0.5256	0.3500	0.5900	0.9953	1.0000	0.0000	0.6796	1.0000	1.56	-25.92	59.6
	0.4865	0.0000	0.9826	0.9999	0.3181	0.9085	0.6976	0.4740	0.6658	0.5429			
	0.6096	0.9997	0.3863	0.4706									
VII	0.7790	0.1309	0.7325	0.9913	0.6683	0.3641	0.7597	0.9994	0.5164	0.2497	1.35	-25.06	54.4
	0.2785	0.6088	0.8325	0.8729	0.1274	0.1717	0.9892	0.6307	0.7907	0.1891			
	0.9626	0.2938	0.5241	0.7151	0.1008	0.5870	0.9995	0.6031	0.4819	0.7547			

Table 9

Current excitation weights, SLL and BWFN for optimal, non-uniformly excited CCAA (Case (b)) using NPSO

Set No.	Current excitation weights for the array elements ( $I_{11}, I_{12}, \dots, I_{mi}$ )									MF	SLL (dB)	BWFN (deg)
III	0.5895	0.9684	0.9999	0.9778	0.9999	0.7511	0.7504	0.4567	0.7547	0.40	-39.38	87.3
	0.7334	0.4502	0.4520	0.5944	0.4278	0.0887	0.4474	0.5906	0.4488			
	0.1376											
V	0.3841	0.5175	0.7782	0.7991	0.7484	0.5967	0.7253	0.7594	0.0000	1.47	-27.78	60.1
	0.8493	1.0000	0.9054	0.0506	0.7521	0.9593	0.4153	0.7860	0.9959			
	0.4315	0.5375	0.3743	1.0000	0.7653	0.3356	0.3897					
VII	0.5478	0.6715	0.7042	0.6778	0.9674	0.5746	0.8762	0.5337	0.8748	1.19	-29.60	52.55
	0.7105	0.0073	0.0273	0.7897	0.5195	0.6712	0.1081	0.0747	0.7765			
	0.3068	0.3318	0.4394	0.8748	0.3860	0.3744	0.3121	0.4117	0.2588			
	1.0000	0.4616	0.2906	0.3932								

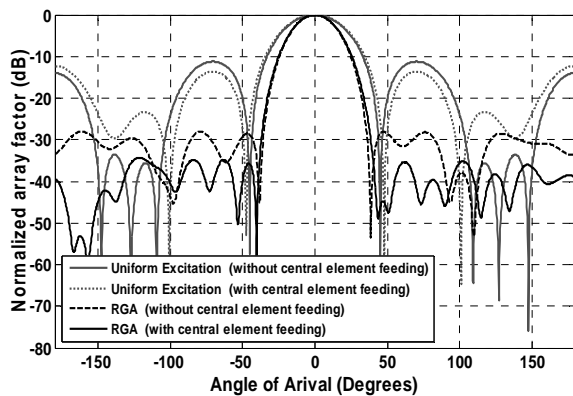


Fig. 8. Radiation patterns for a uniformly excited and RGA based non-uniformly excited CCAA ( $N_1=4, N_2=6, N_3=8$  elements)

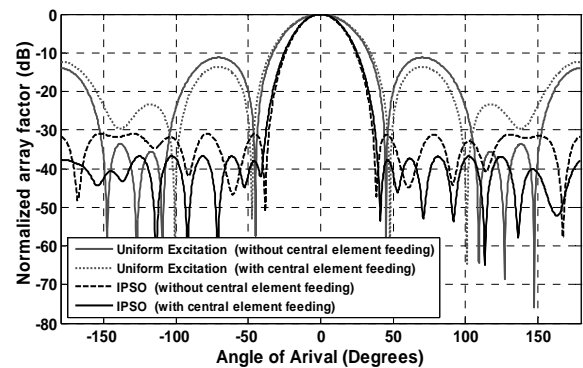


Fig. 9. Radiation patterns for a uniformly excited and IPSO based non-uniformly excited CCAA ( $N_1=4, N_2=6, N_3=8$  elements)



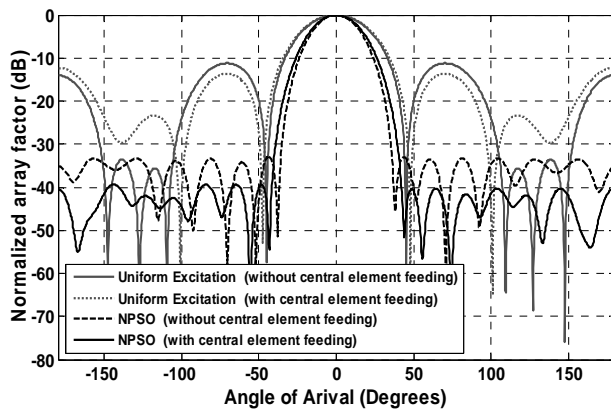


Fig. 10. Radiation patterns for a uniformly excited and NPSO based non-uniformly excited CCAA ( $N_1=4$ ,  $N_2=6$ ,  $N_3=8$  elements).

### 5. B. Comparative effectiveness and convergence profiles of RGA and PSOs

From Tables 4-9, it is observed that as compared to RGA and IPSO, NPSO always yields higher SLL reductions for both without and with central element feeding for all the CCAA sets.

The minimum “Misfitness”  $MF$  values are recorded against the number of iteration cycles to get the convergence profile for each technique as shown in Figs 11-13.

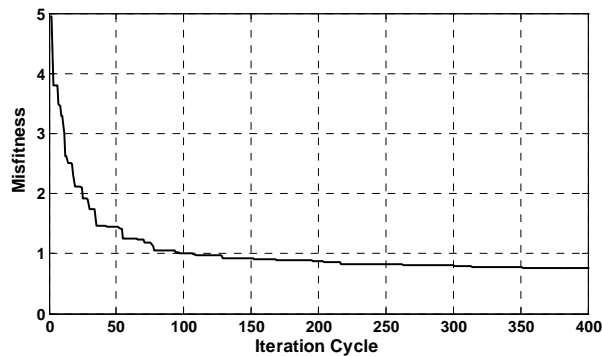


Fig. 11. Convergence curve for RGA in case of non-uniformly excited CCAA ( $N_1=4$ ,  $N_2=6$ ,  $N_3=8$  elements) with central element feeding (Case (b)).

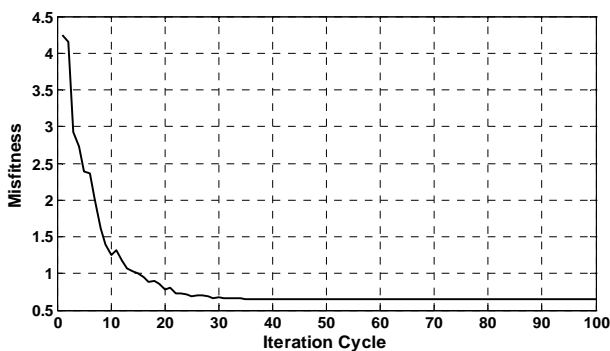


Fig. 12. Convergence curve for IPSO in case of non-uniformly excited CCAA ( $N_1=4$ ,  $N_2=6$ ,  $N_3=8$  elements) with central element feeding (Case (b)).

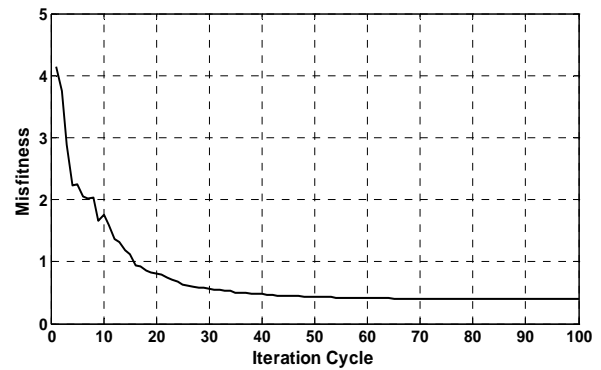


Fig. 13. Convergence curve for NPSO in case of non-uniformly excited CCAA ( $N_1=4$ ,  $N_2=6$ ,  $N_3=8$  elements) with central element feeding (Case (b)).

Tables 4-9 show RGA and IPSO yield suboptimal higher values of grand minimum  $MF$  and NPSO yields optimal (least) grand minimum  $MF$  consistently in all sets and cases. With a view to the above facts, it may finally be inferred that NPSO yields near global optimization. The programming was written in MATLAB 7.5 version on core (TM) 2 duo processor, 3.00 GHz with 2 GB RAM.

### 6. Conclusion

In this paper, the optimal design of a non-uniformly excited CCAA with uniform inter-element spacing and without / with central element feeding has been described using the techniques RGA, IPSO and NPSO. RGA is less robust and yield suboptimal results. IPSO and NPSO technique prove to be faster and more robust techniques. NPSO yields near global optimal current excitation weights and near global minimum values of SLL and BWFN for all sets of CCAA designs. Computational results reveal that the design of optimally and non-uniformly excited CCAA offers a considerable SLL reduction along with the reduction of BWFN with respect to the corresponding non-optimal uniformly excited CCAA. Contribution of the paper is threefold: (i) All CCAA designs having central element feeding yield much more reductions in SLL as compared to the same not having central element feeding, (ii) The CCAA set having  $N_1=4$ ,  $N_2=6$ ,  $N_3=8$  elements along with central element feeding gives the grand minimum SLL (-39.38 dB) as compared to all other sets, which one is thus the grand optimal set among all the three-ring CCAA sets, and (iii) Comparing the performances of the three techniques NPSO shows the best optimization performance as compared to the other two.

### REFERENCES

1. Stearns, C., Stewart, A.: *An investigation of concentric ring antennas with low sidelobes*. In: IEEE Trans. Antennas Propag., vol. 13, no. 6, Nov. 1965, p. 856–863.

2. Das, R.: *Concentric ring array*. In: IEEE Trans. Antennas Propag., vol. 14, no. 3, May 1966, p. 398–400.
3. Goto, N., Cheng, D. K.: *On the synthesis of concentric-ring arrays*. In: IEEE Proc., vol. 58, no. 5, May 1970, p. 839–840.
4. Biller, L., Friedman, G.: *Optimization of radiation patterns for an array of concentric ring sources*. In: IEEE Trans. Audio Electroacoust., vol. 21, no. 1, Feb. 1973, p. 57–61.
5. Huebner, M D. A.: *Design and optimization of small concentric ring arrays*. In: Proc. IEEE AP-S Symp., 1978, p. 455–458.
6. Holtrup, M G., Margulnaud, A., Citerns, J.: *Synthesis of electronically steerable antenna arrays with element on concentric rings with reduced sidelobes*. In: Proc. IEEE AP-S Symp., 2001, p. 800–803.
7. Balanis, C. A.: *Antenna Theory: Analysis and Design*, John Wiley & Sons, New York, 1997.
8. Fallahi, R., Roshandel, M.: *Effect of mutual coupling and configuration of concentric circular array antenna on the signal-to-interference performance in CDMA systems*. In: Progress In Electromagnetics Research, vol. PIER 76, 2007, p. 427–447.
9. Panduro, M. A., Mendez, A. L., Dominguez, R., Romero, G.: *Design of non-uniform circular antenna arrays for side lobe reduction using the method of genetic algorithms*. In: Int. J. Electron. Commun. (AEÜ) vol. 60, 2006, p. 713 – 717.
10. Shihab, M., Najjar, Y., Dib, N. Khodier, M.: *Design of non-uniform circular antenna arrays using particle swarm optimization*. In: Journal of Electrical Engineering, vol. 59(4), 2008, p. 216-220.
11. Haupt, R. L., Werner, D. H.: *Genetic Algorithms in Electromagnetics*, In: IEEE Press Wiley-Interscience, 2007.
12. Dessouky, M., Sharshar, H., Albagory, Y.: *Efficient sidelobe reduction technique for small-sized concentric circular arrays*. In: Progress In Electromagnetics Research, vol. PIER 65, 2006, p. 187–200.
13. Eberhart, R. C., Shi, Y.: *Particle swarm optimization: developments, applications and resources, evolutionary computation*. In: Proceedings of the 2001 Congress on Evolutionary Computation, vol. 1, 2001, p. 81–86.
14. Roy, R., Ghoshal, S. P.: *A novel crazy swarm optimized economic load dispatch for various types of cost functions*. In: Int J Electric Power Energy Syst, vol. 30(4), 2008, p. 242–253.
15. Selvakumar, I., Thanushkodi, K.: *A New Particle Swarm Optimization Solution to Nonconvex Economic Dispatch Problems*. In: IEEE Trans. on power systems, vol. 22(1), February 2007, p. 42-51.
16. Mandal, D., Ghoshal, S. P., Bhattacharjee, A. K.: *Improved Swarm Intelligence Based Optimal Design of Concentric Circular Antenna Array*. In: IEEE Applied Electromagnetics Conference AEMC'09, Dec. 14-16, 2009, Kolkata, p. 1-4.
17. Mandal, D., Ghoshal, S. P., Bhattacharjee, A. K.: *A Novel Particle Swarm Optimization Based Optimal Design of Three-Ring Concentric Circular Antenna Array*. In: IEEE International Conference on Advances in Computing, Control, and Telecommunication Technologies ACT'09, Dec. 28-29, 2009, Trivandrum, p. 385-389.
18. Yao, X., Liu, Y.: *Evolutionary programming made faster*. In: IEEE Trans. Evol. Comput., vol. 3, no. 2, Jul. 1999, p. 82-102.
19. Kilic, O., Nguyen, Q. M.: *Application of artificial immune system algorithm to electromagnetics problems*. In: Progress In Electromagnetics Research B, vol. 20, 2010, p. 1-17.